

## TECHNICAL REPORT

## Simplified protocol for flow cytometry analysis of fluorescently labeled exosomes and microvesicles using dedicated flow cytometer

Vendula Pospichalova<sup>1</sup>, Jan Svoboda<sup>2,3</sup>, Zankruti Dave<sup>1</sup>, Anna Kotrbova<sup>1</sup>, Karol Kaiser<sup>1</sup>, Dobromila Klemova<sup>4</sup>, Ladislav Ilkovic<sup>4</sup>, Ales Hampl<sup>4</sup>, Igor Crha<sup>5</sup>, Eva Jandakova<sup>6</sup>, Lubos Minar<sup>5</sup>, Vit Weinberger<sup>5</sup> and Vitezslav Bryja<sup>1,7\*</sup>

<sup>1</sup>Faculty of Science, Masaryk University, Brno, Czech Republic; <sup>2</sup>Cytometry and Microscopy Facility, Institute of Microbiology, Academy of Sciences of the Czech Republic, Prague, Czech Republic; <sup>3</sup>Bio-port Europe, Svinare, Czech Republic; <sup>4</sup>Faculty of Medicine, Masaryk University, Brno, Czech Republic; <sup>5</sup>Department of Obstetrics and Gynecology, Faculty Hospital Brno, Brno, Czech Republic; <sup>6</sup>Department of Pathology, Masaryk University and University Hospital Brno, Brno, Czech Republic; <sup>7</sup>Institute of Biophysics, Academy of Sciences of the Czech Republic, Brno, Czech Republic

Flow cytometry is a powerful method, which is widely used for high-throughput quantitative and qualitative analysis of cells. However, its straightforward applicability for extracellular vesicles (EVs) and mainly exosomes is hampered by several challenges, reflecting mostly the small size of these vesicles (exosomes: ~80–200 nm, microvesicles: ~200–1,000 nm), their polydispersity, and low refractive index. The current best and most widely used protocol for beads-free flow cytometry of exosomes uses ultracentrifugation (UC) coupled with floatation in sucrose gradient for their isolation, labeling with lipophilic dye PKH67 and antibodies, and an optimized version of commercial high-end cytometer for analysis. However, this approach requires an experienced flow cytometer operator capable of manual hardware adjustments and calibration of the cytometer. Here, we provide a novel and fast approach for quantification and characterization of both exosomes and microvesicles isolated from cell culture media as well as from more complex human samples (ascites of ovarian cancer patients) suitable for multiuser labs by using a flow cytometer especially designed for small particles, which can be used without adjustments prior to data acquisition. EVs can be fluorescently labeled with protein- (Carboxyfluoresceinsuccinimidyl ester, CFSE) and/or lipid- (FM) specific dyes, without the necessity of removing the unbound fluorescent dye by UC, which further facilitates and speeds up the characterization of microvesicles and exosomes using flow cytometry. In addition, double labeling with protein- and lipid-specific dyes enables separation of EVs from common contaminants of EV preparations, such as protein aggregates or micelles formed by unbound lipophilic styryl dyes, thus not leading to overestimation of EV numbers. Moreover, our protocol is compatible with antibody labeling using fluorescently conjugated primary antibodies. The presented methodology opens the possibility for routine quantification and characterization of EVs from various sources. Finally, it has the potential to bring a desired level of control into routine experiments and non-specialized labs, thanks to its simple bead-based standardization.

**Keywords:** *exosomes; microvesicles; extracellular vesicles; quantification; flow cytometry; fluorescent labeling; CFSE; lipophilic styryl dye; ascites*

\*Correspondence to: Vitezslav Bryja, Faculty of Science, Institute of Experimental Biology, Masaryk University, Kamenice 753/5, building A36, CZ-625 00 Brno, Czech Republic, Email: bryja@sci.muni.cz

Received: 23 July 2014; Revised: 3 March 2015; Accepted: 4 March 2015; Published: 31 March 2015

**E**xosomes (exs) are cell-derived vesicles that are present in numerous biological fluids and also in conditioned media (CM) of cell cultures. Exs originate as multivesicular bodies within the endosomal compartment of cells. However, cells also secrete other

types of extracellular vesicles (EVs), for example, microvesicles (MVs), that are larger than exs and originate from plasma membrane (1). All types of EVs are composed of various protein and lipid species reflecting the status and the cell of origin, and contain various cargo (DNA,

RNA, protein) [reviewed in (2,3)]. EVs, and particularly exs, are an important, yet only recently appreciated, mode of intercellular communication (4) and thus have attracted growing interest of the basic researcher community. Moreover, they have also gained lots of attention from clinical researches as increasingly recognized high-potential biomarkers of several diseases including cancer (5), as well as possible therapeutic vehicles (6).

The exosomal field suffers from the lack of an easy, fast, and reliable method for quantification and characterization of these nanosized vesicles on a single particle level. Currently, characterization of exs is mainly based on the level of total amount of proteins and/or lipids in bulk isolates from biological samples. However, the methods used for bulk isolates, such as mass spectrometry or western blotting (WB), are rigid because they cannot dissect, whether the observed difference in protein/lipid abundance reflects the change in number of exs or in their composition mostly due to the absence of invariant “household” exs markers (7). Recent developments of nanoparticle tracking analysis (NTA) (8) allow for enumerating and also sizing of individual exs on the basis of Brownian motion. However, this light scattering–based approach also harbors several inherent disadvantages, for example, the ultimate need for multiple measurements of samples at different dilutions and different settings due to low dynamic range of the camera, which does not cover the range of 5 order of magnitude difference between the light scattered by smallest and largest EVs (9). Moreover, NTA technology is nowadays often used to detect only size and not to discriminate the composition of the particles (such as protein aggregates, micelles and lipoprotein particles, or abundance of a particular protein) thus often leading to overestimation of EV numbers. These potential errors in enumeration of EVs can only be partially limited by standardization of NTA measurements (10).

To ease the flow cytometry (FC; in further text also refers to “flow cytometer,” that is, instrument used in flow cytometry) analyses, exs are often bound to beads that provide larger surface and more scattered light. However, this approach is inconvenient for subsequent use of exs for functional studies. Moreover, the detection is largely dependent on the abundance/availability of antigen on the exs, which is recognized by the antibody coupled to the beads reflecting both *pro et contra* associated with high specificity of antibodies (11). Currently, the only reliable protocol available for free exs and direct FC analysis is a protocol for multiparameter FC analysis developed by research group of Prof. Marca Wauben (7,12). It allows for a high-resolution quantitative and qualitative analysis of individual cell-derived vesicles using an optimized configuration of the commercially available high-end FC (BD Influx). This extremely useful and exemplary protocol, though, demands an experienced

FC operator capable of manual hardware adaptations with adjustments and calibration of the FC before use. Moreover, the exs labeling part of the experimental procedure, which yields multiple highly purified populations of exs, is also rather time and labor extensive and therefore as such may be discouraging for users in clinical labs or labs that do not highly specialize in the exs research.

Here, we present a simplified protocol for FC analysis of EVs using UC followed by a sucrose cushion purification step and simple fluorescent labeling step without additional washes requiring prolonged UC. The FC characterization is performed using a dedicated FC, where no adjustments prior to measurements are needed. By term dedicated FC [adopted from (9)], we specifically refer to Apogee A50 Micro (Apogee Flow Systems, Hertfordshire, UK), a FC specially developed for analysis of small particles (9,13,14).

## Materials and methods

### Cell culture and labeling by CFSE

HEK293 cells were cultured in DMEM supplemented with 10% FBS, 2 mM L-glutamine, 50 units/ml penicillin, and 50 units/ml streptomycin. Kuramochi and Ovsaho cell lines were cultured in RPMI 1640 supplemented with 10% FBS, 2 mM L-glutamine, 50 units/ml penicillin, and 50 units/ml streptomycin. For isolation of exs, cells were harvested with 0.05% trypsin/EDTA, washed twice in PBS and plated at 50% confluence onto fresh plates into RPMI 1640 or DMEM supplemented with vesicle-free 10% FBS, 2 mM L-glutamine, 50 units/ml penicillin, and 50 units/ml streptomycin. Supernatants were collected 24–48 h later.

Vesicle-free medium was prepared as described in Current Protocol in Cell Biology (15). In brief, medium was supplemented by 20% FBS, 4 mM L-glutamine, 100 units/ml penicillin, and 100 units/ml streptomycin and centrifuged at  $100,000 \times g$ , 4°C in SW28 rotor overnight (16–18 h). Supernatant was filter sterilized using 0.22 µm PVDF filter and 1 time diluted with DMEM or RPMI 1640 to reach the 10% FBS, 2 mM L-glutamine, 50 units/ml penicillin, and 50 units/ml streptomycin concentrations. To harvest fluorescently labeled EVs, CFSE (Carboxyfluoresceinsuccinimidyl ester, e-Bioscience) (or DMSO as diluent control) was added to final concentration 2–20 µM into vesicle-free cell culture medium at the time of seeding of the cells, which was typically onto 150 mm dish in 35 ml of culture media.

### Ascites collection

Primary ascites of ovarian cancer patients were collected at the Department of Obstetrics and Gynecology, Faculty Hospital Brno, Czech Republic, under the informed consent of patients and IRB protocol of Vitezslav Bryja

(MUNI/M/1050/2013) approved by the Ethics Committee of Faculty Hospital Brno.

### Isolation of cells and EVs

Exs and MVs were isolated according to slightly modified Current Protocol in Cell Biology (15). A scheme of the isolation protocol is given in Fig. 2. In detail, cell culture media or ascites were collected and transferred to 50-ml centrifugation tubes. Live cells were pelleted upon 5 min centrifugation at  $200 \times g$  at  $4^\circ C$  (designated P 0.2 – P, pellet, 0.2 – relative centrifugation force (RCF) in thousands of g). P 0.2 fraction from ascites usually contains red blood cells (RBC), which were removed by washing with ACK lysis buffer (150 mM  $NH_4Cl$ , 10 mM  $KHCO_3$ , 1 mM EDTA) and subsequent pelleting. The RBC removal step was repeated several times if necessary until both the pellet and the supernatant were clear (without the red traces of contaminating hemoglobin). Supernatants after live cell pelleting (S 0.2) were transferred to new 50-ml centrifugation tubes and centrifuged at  $1,500 \times g$  at  $4^\circ C$  for 10 min to remove cell debris (P 1.5). S 1.5 was transferred to 38-ml thinwall polyallomer SW28 UC tubes (Beckman Coulter) and centrifuged at  $14,000 \times g$  (8,800 rpm for SW28 rotor – Beckman Coulter) for 1:10 h at  $4^\circ C$  to isolate MVs (P 14). The P 14 was resuspended in filtered (0.22  $\mu m$  PVDF filter) PBS and the centrifugation step was repeated to wash MVs from non-specifically adhered proteins. S 14 was optionally filtered using 0.22  $\mu m$  PVDF filter to remove any contaminating MVs (larger than 220 nm) and the S 14 filtrate or S 14 was transferred to fresh 38-ml thinwall polyallomer SW28 UC tube and centrifuged for  $100,000 \times g$  (23,500 rpm for SW28 rotor) at  $4^\circ C$  for 3:10 h using Optima XPN 90K Ultracentrifuge (Beckman Coulter). Sucrose cushion (4 ml) (30% sucrose in 20 mM Tris pH 7.6 in  $D_2O$ , filter sterilized) was pipetted into new SW28 tubes. S 100 was completely removed and P 100 was resuspended in 30 ml of filtered PBS, gently laid onto sucrose cushion, not to disturb the interface and UC for  $100,000 \times g$  at  $4^\circ C$  for 1:10 h. Approximately 6 ml of cushion and PBS (to ensure no exs are lost at the interface) was collected from the side of tube using 18-G needle fitted to 10 ml syringe, transferred to fresh tube, mixed with 30 ml filtered PBS and ultracentrifuged (1:10 h,  $100,000 \times g$ ,  $4^\circ C$ ). The supernatant was discarded and pellet of exs was resuspended in 100–200  $\mu l$  of filtered PBS for further analysis.

### Fluorescent labeling of exs prior to the measurement

Exs and MVs were isolated from ascites or CM as described above using UC and sucrose cushion. To fluorescently label EVs proteins, the isolated EVs were incubated in 100 nM to 10  $\mu M$  CFSE (e-Bioscience) for 30 to 45 min at  $37^\circ C$  in the dark. Specifically, for measurements in triplicate, 500- $\mu l$  samples were prepared in 1.5 ml tubes by diluting the isolated exs in 495  $\mu l$  of filtered PBS and adding 5  $\mu l$  of 10 to 1,000  $\mu M$  CFSE (or DMSO as a diluent control), prepared according to manufacturer's

instructions. After its cleavage of acetate groups by esterases (16), which are present in cells as well as in secreted EVs, CFSE has a peak excitation of 494 nm and peak emission of 521 nm (17), which is ideally measured using 488-nm (blue) laser excitation and 535/35 band pass filter for detection. Alternatively, for fluorescent labeling of exs lipids, the isolated exs were incubated in 100 ng/ml to 10  $\mu g/ml$  FM 1-43FX or FM 4-64FX (Life Technologies) for 10 min at  $37^\circ C$  in the dark. Specifically, for measurements in triplicate, 500- $\mu l$  samples were prepared by diluting the isolated exs in 495  $\mu l$  of filtered PBS and supplementing it with 5  $\mu l$  of 10 to 1,000  $\mu g/ml$  FM dye (or HBSS as a diluent control), prepared according to manufacturer's instructions. After incubation at  $37^\circ C$ , tubes were gently flicked, liquid collected at the bottom of the tubes and immediately subjected to measurements by FC by inserting the 1.5-ml tubes into the moving arm of the device. Of importance, unbound fractions of CFSE, FM 1-43FX, or FM 4-64FX do not seem to interfere with the FC measurements, unlike the unbound fractions of PKH67 and Di- dyes, which need to be separated by UC in sucrose gradient [(7), data not shown].

### Labeling of exs with antibodies

Isolated exs were labeled according to (7). In short, isolated exs were incubated for 60 min with 10  $\mu l$  of mouse anti CD63-PE (MEM-259, Exbio, 1P-343). Prior to data acquisition, the samples were diluted with 480  $\mu l$  0.22  $\mu m$  filtered PBS (final dilution 1:25). PE conjugated antibody of unknown specificity (MOPC-21, Exbio, 1P-632) was used as negative IgG1 isotype control for background fluorescence. For double labeling with CFSE and anti EpCAM antibody, exs were incubated for 45 min at  $37^\circ C$  with anti EpCAM-APC (e-Bioscience, 17-5791-80) or isotype control (e-Bioscience, 17-4321-81) antibody and 1  $\mu M$  CFSE.

### Dedicated FC instrument settings

Data were obtained using 2 individual Apogee A50/Micro flow FCs equipped with 50 mW 405-nm (violet), 488-nm (blue) and 638-nm (red) lasers. Parameters in the Control panel were set to sheath pressure of 150 mbar and number of flush cycles to 4. Peak is a preferred parameter to area for light scatters (LSs) and fluorescence channels, as it corresponds better to submicron particles than the area. Particles with size several times smaller than the focused laser beam are being exposed to the light continuously across their path through the beam. Thus, the area of the pulse corresponds more to the length of the path (or the exposure time), than to the size of the particle. The peak value of the pulse should remain consistent across the particle path through the focused laser beam and should only reflect the scattering properties of the particle, with small or no regard to the length of the path (or exposure time) (18).

On each day of measurements, the FC performance was first verified using a reference bead mix. The reference bead mix (*Apogee Mix*, Apogee Flow Systems, cat#1493) composed of a mixture of plastic spheres with diameters of 180 nm, 240 nm, 300 nm, 590 nm, 880 nm, and 1,300 nm with a refractive index (RI) of 1.42, and 110-nm and 500-nm green fluorescent (excited by blue laser) beads with RI of 1.59 (latex) were used. These beads were used to assess the FC's light scattering and fluorescence performance (both sensitivity and resolution). This can easily and quickly inform the user, whether the FC at current settings is capable of quality measurements of EVs. These beads were run several times during the acquisitions and at the end of the day to control the quality of recorded data among samples and stable FC performance during all measurements. Reference bead mix was used to set the PMT voltages and the thresholds for light scattering. Furthermore, as 2 populations of these beads are fluorescent in green channel, they were used to set the PMT voltages and the thresholds for fluorescent threshold triggering in parallel. All measurements were performed in log mode. The noise levels in PMT panel were kept below 1 at all parameters, ideally below 0.5.

Use of 405-nm laser is preferable for determination of light scattering, as it results in more scattered light and thus better resolution and sensitivity at light scattering detectors than 488-nm laser. However, as we used fluorescence threshold triggering in the blue part of spectrum, we measured the samples with both 405-nm and 488-nm lasers on. Importantly, we have not recorded photobleaching of the fluorescent particles with 405-nm laser when we compared the cytograms recorded with 405 nm, 488 nm, or both lasers. It is highly advisable to check regularly on Live camera window, whether the stream of particles is directed to the middle of laser beam. This indicates that there is no air bubble stuck in the tubing. In case of distorted particle stream, extensive cleaning can be applied to the tubing by selecting Clean valve button in the Control panel. If cleaning the valve does not correct the stream flow, it is preferable to replace the sheath fluid (dH<sub>2</sub>O water).

#### FC data acquisition

After FC calibration by reference bead mix, the FC tubing was washed by 10% bleach to remove any particles which might have had adhered within the tubing. This wash was performed at sample flow rate 10.5–15  $\mu\text{l}/\text{min}$  with 130- $\mu\text{l}$  sample volume for 120 s. To remove the bleach, further wash was performed similarly with 0.22  $\mu\text{m}$  filtered PBS. Such bleach and PBS washes were included after every positive sample, to exclude carryover of fluorescently positive events (EVs/fluorescent dye) between samples. The cleanness of tubing was verified by subsequent acquisition of filtered PBS sample at sample flow rate 0.75 or 1.5  $\mu\text{l}/\text{min}$  with 130- $\mu\text{l}$  sample volume for 120 s. This very low sample flow rate 0.75 or 1.5  $\mu\text{l}/\text{min}$

(0.75  $\mu\text{l}/\text{min}$  is the minimum) was used for all measurements and the time of acquisition was held constant for all samples, at least 120 s (or until the data buffer was full – up to 5,000,000 events), to yield enough events. Samples (500- $\mu\text{l}$ ) were just enough for measurements of 130- $\mu\text{l}$  per sample in triplicates, leaving approximately 20- $\mu\text{l}$  sample volume for data acquisition (more than 10 min at flow rate 1.5  $\mu\text{l}/\text{min}$ ), as roughly 110  $\mu\text{l}$  encompass the dead volume of tubing of the FC.

#### Western blotting

Parental cells were lysed in NP40 lysis buffer (50 mM Tris pH 7.4, 150 mM NaCl, 1 mM EDTA, 0.5% NP40) supplied with 1  $\times$  Complete protease inhibitor mix (Roche), and 1  $\times$  Phosphatase inhibitor cocktail (Calbiochem). Lysates were spun down (16,000  $\times$  g, 10 min, 4°C). The total protein concentration was determined using DC™ Protein Assay (Bio-Rad). The protein lysates and isolated exs were mixed with 2  $\times$  Laemmli buffer and separated according to their molecular mass on 10–15% SDS-PAGE and transferred to Immobilon-P Membrane (Millipore). WB and antibody detection was performed as described previously (19). The antibodies used were rabbit anti Alix (gift from Pascale Zimmermann), mouse anti CD63 (MEM-259, Exbio, 11-343), mouse anti Golgin A1 (Invitrogen, A21270), mouse anti Hsc70 (Santa Cruz, sc-24), and rabbit anti Tsg101 (Sigma Aldrich, HPA006161).

#### TEM and immunogold labeling

For negative contrasting 10- $\mu\text{l}$  drops of exs in PBS were adsorbed at activated formvar membrane coated HF35Cu with carbon EM grids (Pyser–SGI Limited) for 15 min, stained with 2% ammonium molybdate for 20 s at RT, washed with dH<sub>2</sub>O water and imaged using transmission electron microscopy (TEM) Morgagni 268D (FEI) equipped with Mega ViewIII (Soft Imaging System) at 70 kV.

For immunogold labeling, isolated exs were mixed 1:1 with freshly prepared 8% paraformaldehyde and fixed for 10 min at RT. Then they were resuspended in 5 ml PBS and ultracentrifuged onto activated formvar membrane coated HF35Cu with carbon EM grids (Pyser–SGI Limited) placed at the bottom of the SW55Ti rotor UC tubes (Beckman Coulter) for 1 h at 100,000  $\times$  g, 4°C. Grids were blocked by 0.5% BSA + 0.1% Tween 20 in PBS for 30 min, incubated with primary antibody anti CD63 (MEM-259, Exbio, 11-343, dilution 1:200 in 0.5% BSA in PBS) overnight at 4°C, washed 3 times for 15 min with 0.5% BSA in PBS, then incubated with secondary anti mouse antibody conjugated with 10-nm gold particles (G7652, Sigma Aldrich, dilution 1:40 in PBS) for 2 h at RT, washed 3 times for 15 min in PBS and once with dH<sub>2</sub>O. After staining with 2% ammonium molybdate for 20 s at RT, grids were washed with dH<sub>2</sub>O water and imaged using

TEM Morgagni 268D (FEI) equipped with Mega ViewIII (Soft Imaging System) at 70 kV.

### Statistical analysis

Graph visualization, data transformation, linear regression analysis, and concentration calculations were performed using Prism (version 5.0, GraphPad Software) and Microsoft Office Excel (version 2010, Microsoft).

## Results and discussion

### Challenges of FC of EVs and the ways to overcome them

We have decided to use FC to precisely quantify and characterize exs and MVs. FC is a powerful method for the high-throughput analysis of small particles which, however, has its limitations. Specifically, there are 2 main issues, which complicate FC-based analysis of EVs. First, the size of the vesicles ranges from 80 up to more than 1,000 nm, with the majority formed by exs, which are smaller than  $\sim 200$  nm. The vast majority of conventional FC has the minimal detection limit for light scattering in a range of 200–500 nm (20). In addition, the conventional FC cannot discriminate accurately between particles that differ by less than 100–200 nm in diameter (21). Second, LS-based detection of EVs smaller than 200–300 nm is severely compromised by overlapping noise derived from optics, electronics, and buffers used.

To overcome these limitations we used a FC, which is optimized for the detection of small particles. In the further text we refer to this instrument as the “dedicated FC.” Conventional FCs use forward scatter (FSC), which detects the amount of light scattered at small angles ( $0.5\text{--}15^\circ$ ) and side scatter (SSC), which detects the light scattered at the angle of  $90^\circ$ . FSC is commonly interpreted as an estimate of size for objects larger than 500 nm, for example, cells, whereas SSC is used as a measure of their internal complexity (18). The dedicated FC builds on the fact that objects with sizes close to the observing light wavelength, such as exs, scatter significantly more light at larger angles ( $15\text{--}150^\circ$ ) due to diffraction (18,22). Thus, the dedicated FC uses alternative LSs such as SALS (small angle light scatter), MALS (middle angle light scatter), and LALS (large angle light scatter) for determination of light scattering. SALS, MALS, and LALS can be used for relative particle sizing and the latter also for internal complexity of the particles to limited extent.

Dedicated FC can thus, in principle, distinguish particles with the optical properties and size similar to exs and thus MVs as well. Our testing of the reference bead mix confirmed that dedicated FC is suitable for small particle measurements giving exceptional small particle sensitivity (approximately 100-nm latex beads) and resolution (difference of latex bead size in tens of nanometers) (Fig. 1a). Silica beads were used as a size reference because they

have a RI of approximately 1.42 which is closer to the RI of biological particles [approximately 1.4 for cells (23) and  $1.40 \pm 0.02$  for EVs (9)] than latex particles [RI of 1.59 (24)].

The reference bead mix used in our experiments is a mixture of fluorescent and non-fluorescent spheres with diameters from 110 to 1,300 nm. To assess the suitability of individual LS detectors for detection of small particles, we have used the reference bead mix to assess the coefficient of variation (CV) of the SALS, MALS, and LALS detectors (reflecting the size of particles). With the manufacturer’s default settings, we did not observe  $CV > 10\%$ ; actually in most cases CV was below 3%. At the default manufacturer’s setting, the best resolution and sensitivity for smallest particles was obtained on SALS (Fig. 1a). However, it should be noted that the device settings can be fine-tuned by experienced FC operators for best performance at LALS and/or MALS and yield better resolution and sensitivity for the expected exs populations (we have used this setting in Fig. 6c). Nevertheless, all other measurements in this study (shown in Figs. 1, 3–5, 6d) were obtained using the default settings to better illustrate the situation in non-specialized labs.

### Reduction of noise

Data shown in Fig. 1a suggest that dedicated FC is able to detect particles with the properties – size and RI – very similar to MVs and exs. The detection of EVs by FC is, however, in parallel hampered by high level of noise. In the next step, we thus decided to identify and subsequently eliminate factors, which increase the noise and may interfere with the interpretation of the analysis.

First, we found it critical to acquire the data at a low flow rate (0.75 or 1.5  $\mu\text{l}/\text{min}$ ) for good LS resolution as well as for the accurate discrimination between non-fluorescent noise and fluorescent signals. This is likely because higher flow rates increase the diameter of the sample stream and allow the particles to move outside the center of the laser spot, yielding lower intensity of light scattering and fluorescent signals and increasing the CVs accordingly.

Second, we tested the effect of 0.22  $\mu\text{m}$  filtration of PBS, which is used to dissolve the EV samples. As shown in Fig. 1b, use of filtered PBS in all steps of FC measurements greatly – 5.8 times – reduces the number of small events recorded by the FC (Fig. 1b). In the next experiments we took advantage of filtered PBS and used this solution during the calibration of the instrument for the fluorescent application in a way that the event rate was not higher than 2 events/ $\mu\text{l}$  for 0.22  $\mu\text{m}$  filtered PBS in fluorescently positive region (quadrants A and B) (Fig. 1b).

Third, we have attempted to reduce the noise by gating events of interest using combination of 2 LSs. When using the reference bead mix, it is possible to gate on the beads

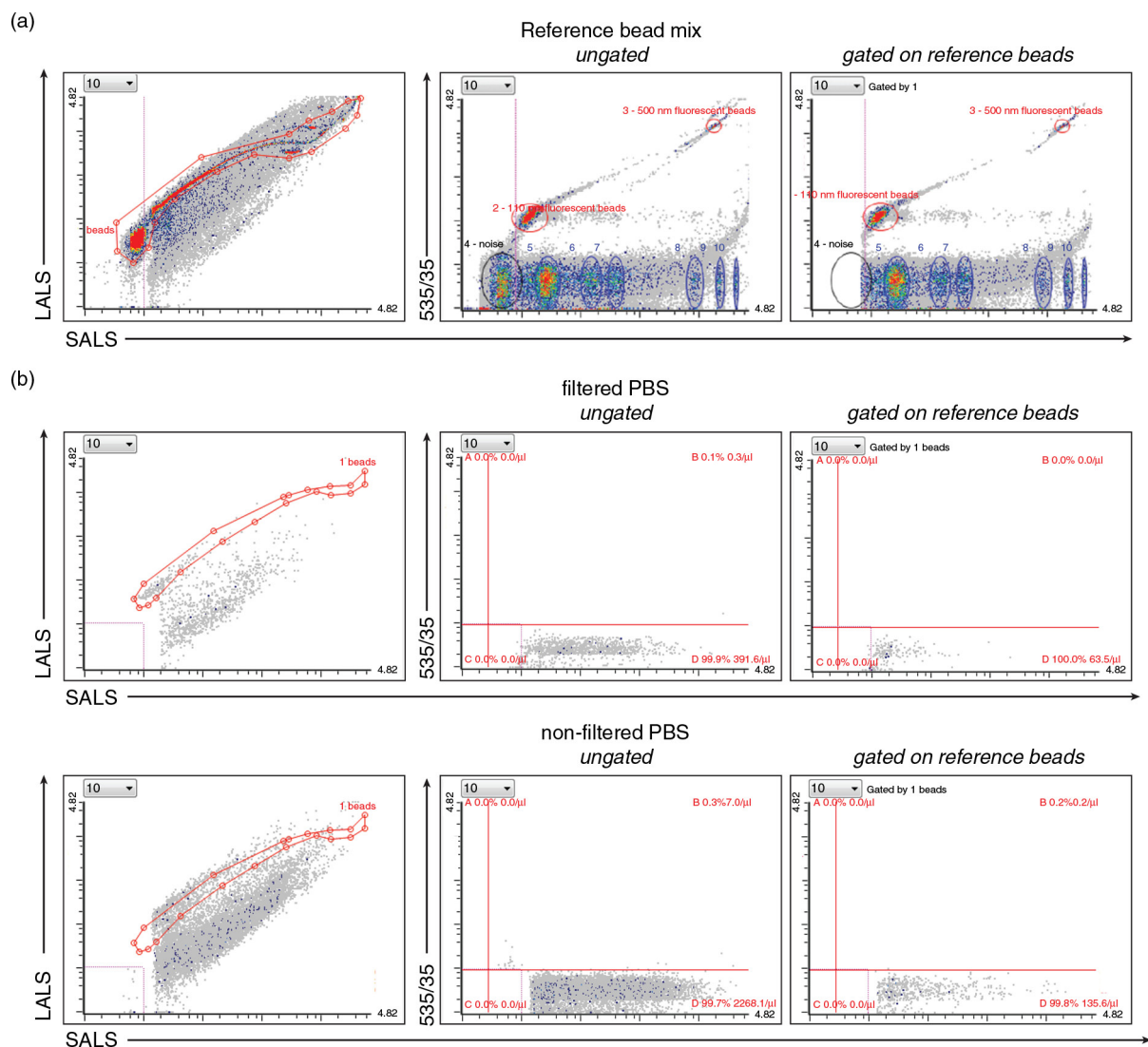


**Fig. 1.** Setting up the dedicated flow cytometer (FC). (a) The resolution of the reference bead mix indicates the FC's performance in light scattering at default settings. Left cytogram shows small angle light scatter (SALS) versus large angle light scatter (LALS). Right cytogram depicts SALS versus 535/35 (green fluorescence triggering) channel. Six populations with refractive index (RI) 1.42 (blue ellipses) and two green fluorescent populations (110 nm and 500 nm) with RI 1.59 (red ellipses) were resolved from the instrument noise (black ellipse). The original outputs from Histogram software (Apogee Flow Systems) are shown. (b) Use of filtered (0.22 PVDF filter) PBS is highly recommended for all FC measurements. Left panels, diagrams show SALS versus LALS cytograms, middle panels show SALS versus 535/35 for ungated population, while right panels represent cytograms events gated on ROI 1 (beads) of reference bead mix in the SALS versus LALS cytograms. Gating on ROI 1 eliminates very rare false positive events in upper left quadrant B in case of PBS, but also results in significant decrease of fluorescently positive exs detected in this quadrant and thus is not used in following experiments. On contrary, employing the filtered PBS significantly decreased the total number of presumably noise events recorded in quadrant D, as well as non-specific events in quadrant B.

[region of interest 1 (ROI 1)] in the SALS versus LALS (Peak-Peak) cytogram and quantify the number of un-specific events in the next SALS versus 535/35 cytogram (Fig. 1b; middle panels – no gating; right panels – ROI 1 gated). We assumed that analysis of EVs may profit from such gating because of the bead size and RI resembling exs. Note that ROI 1 spreads to the noise region as well, to include any potential exs which scatterless light than 110-nm beads. However, reduction of noise was negligible

(Fig. 1b) and on the opposite side restriction of events to ROI 1 significantly reduced the number of detected exs in subsequent experiments. Therefore, we present the data of ungated populations in following Figs. 3–6.

#### Purification of exs from cell culture media and patient ascites for FC analysis

The results shown in Fig. 1a suggested that dedicated FC represents a method with the potential to directly, rapidly,

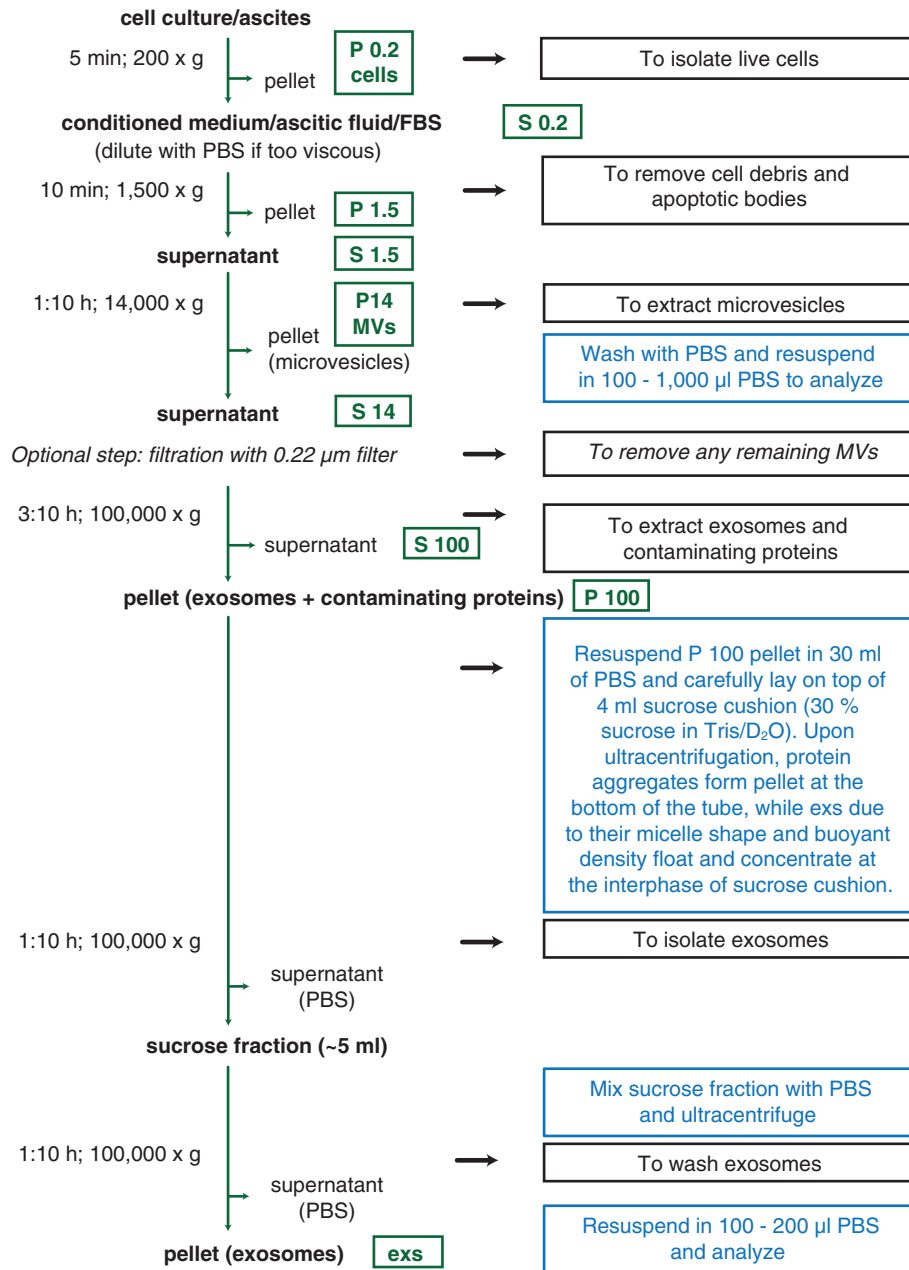


**Fig. 2.** Isolation of microvesicles (MVs) and exosomes (exs) by ultracentrifugation (UC) and sucrose cushion. A schematic representation of protocol used to isolate extracellular vesicles (EVs). Black boxes describe the purpose of each centrifugation step, blue boxes contain additional instructions/explanation. Optional filtration step is indicated by italics. Green boxes depict fraction after centrifugation at relative centrifugation force (RCF) indicated by number (in thousands × g). P, pellet; S, supernatant.

and precisely quantify exs and other EVs. In the next step we decided to validate this assumption on real samples and to implement this step into possibly routine workflow for the isolation and analysis of exs and MVs.

As the first step in the workflow, we have chosen a suitable purification method – that is, a method which is relatively fast and unbiased. As such we decided to use a protocol based on UC. UC is still regarded as the gold standard for isolation of exs for basic research (25).

This is despite the increasing availability of other methods because UC-based methods collect in an unbiased way the exs, which may vary morphologically, biochemically, and functionally. Separation of exs by sedimentation only (=downward displacement) during UC is not sufficient, although it is still used by many labs. Separation of exs from other particulate material can be guaranteed only by floatation (=upward displacement) (26). Upward displacement can be performed either as an isopycnic

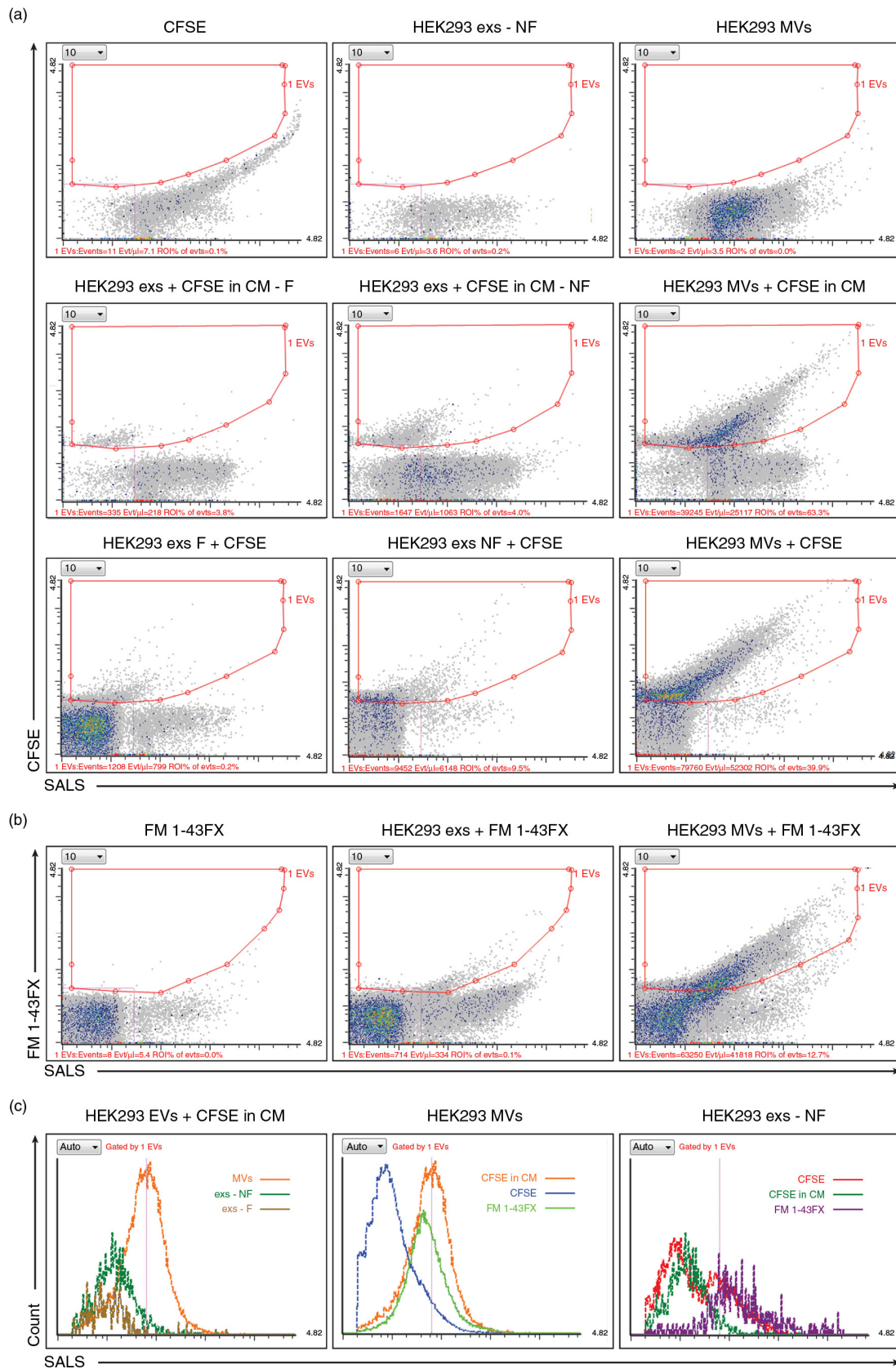


Fig. 3. (Continued)



centrifugation where floatation in sucrose gradient is used or as centrifugation into the sucrose cushion. Isopycnic centrifugation yields high purity exs, but is technically more demanding and more time consuming (16–22 h) (11). In comparison to isopycnic centrifugation, sucrose cushion has several advantages for use in our workflow: (a) it is rapid (only 70 min); (b) the 30% sucrose in D<sub>2</sub>O has a density of 1.19–1.2103 g/ml, which enables it to concentrate the majority of the exs (typical buoyant density 1.10–1.19 g/ml) in single low-volume fraction and to increase purity of exs, due to the formation of a continuous minigradient between 1.10 and 1.19 g/ml at the interphase between cushion and PBS (27); and (c) given the density of D<sub>2</sub>O is 1.11 g/ml, significantly less sucrose is required to reach the cushion density of 1.21 g/ml than if prepared in H<sub>2</sub>O, thus reducing potential hyperosmotic stress for exs (27).

Based on the arguments above we have used the UC and sucrose cushion-based protocol (schematized in Fig. 2) to isolate EVs from several sources. We purified MVs and exs from CM of 3 different cell lines – HEK293, Kuramochi, and Ovsaho (last 2 derived from high-grade serous ovarian cancer) and from primary patient samples. We have chosen samples of malignant ascites, that is, excessive fluid accumulated in the peritoneum of patients with high-grade serous ovarian cancer (28), which contains both cells, including ovarian cancer cells and leukocytes, and numerous EVs of unknown function.

MVs and exs produced by cell lines and from primary human material can be easily detected by a dedicated FC.

To distinguish EVs from the noise, we first stained them with the fluorescent dyes. Two different green fluorescent dyes – protein-specific (CFSE) and lipid-specific (FM 1-43FX) – were tested. The initial comparison was performed on MVs and exs produced by HEK293 cells into the culture media. EVs, labeled fluorescently by CFSE during cell culture (HEK293 exs+CFSE in CM) or prior to measurements by CFSE (HEK293 exs+CFSE) or FM 1-43FX dye (HEK293 exs+FM 1-43FX) were isolated using protocol outlined in Fig. 2 and subsequently analyzed by dedicated FC (Fig. 3) and by TEM in parallel (Fig. 4a).

The gates corresponding to fluorescently labeled EVs (ROI 1 in Fig. 3a–b) were set based on the acquisition of the free dyes (unbound to EVs) at highest final con-

centrations used for labeling and non-labeled EVs. For 10 µg/ml FM 1-43FX measurement, we allowed a maximum of 6 events/µl in ROI 1 when ungated (Fig. 3b). Using this setting, 10 µM CFSE label yielded a maximum of 8 events/µl, 0.22 µm filtered PBS ≤1 event/µl and similar events/µl were recorded for non-fluorescent EVs (Fig. 3a). MVs are clearly larger than exs, as evidenced by SALS histogram (Fig. 3c). Moreover, when S 14 was filtered prior to 100,000 ×g UC step to remove all residual MVs and aggregated exs (designated as –F), it resulted in decreased number of more scattering EVs (Fig. 3) but also into significant loss of EVs detected, when compared to exs isolated from parallel samples when the 0.22 µm filtration step of S14 was not performed (designated as –NF). Thus, we included the filtration only as an optional step into the purification protocol (Fig. 2). We have noted the difference in ROI 1 population characteristics when labeled by lipophilic dye (membrane surface labeling) in comparison with luminal labeling by protein-specific dye CFSE. The surface labeling results in seemingly larger EVs as they were more shifted in SALS than if post stained with CFSE (Fig. 3). CFSE<sup>+</sup> exs show more discrete fluorescent population when labeled during the biogenesis of exs (HEK293 exs+CFSE in CM) than population labeled by CFSE post isolation (HEK293 exs+CFSE) (Fig. 3a). Importantly, fluorescent staining of MVs and exs from HEK293 CM did not affect exosomal morphology/size as assessed by TEM (Fig. 4a). The morphological characteristics of EVs isolated from HEK293 cells with or without CFSE in culture medium were unchanged and sizes corresponded to the expected ~80–200 nm in diameter, whereas the MVs were much larger – hundreds of nm (Fig. 4a).

Next, we tested labeling of more complex exosomal mixtures isolated from human samples – malignant ascites of ovarian cancer patients. In Fig. 4b, we also demonstrate that these exs can be labeled by CFSE or FM 1-43FX dyes prior to FC data acquisition. Filtration with 0.22 µm filter resulted again in significant loss of recorded events; however, in such exs sample isolated from a complex mixture, not all fluorescent events with high SALS value could be eliminated by filtration, as these may also represent aggregates formed during labeling. In non-filtered samples, we observed contamination of the sample by

**Fig. 3.** FC analysis of EVs isolated from cell culture media. (a) EVs were labeled by protein-specific (CFSE) fluorescent dye either during their genesis in cells (HEK293 exs+CFSE in conditioned media(CM)) – middle panel, or just prior to measurements (HEK293 exs+CFSE) – lower panel. The upper panel consists of negative control samples – CFSE-only, HEK293 exs-only, HEK293 MVs-only. (b) EVs were labeled by lipid-specific (FM 1-43FX) dye prior to measurements (HEK293 exs or MVs+FM 1-43FX). FM 1-43FX-only represents negative control sample. (a–b) SALS versus CFSE or FM 1-43FX (both green fluorescence) cytograms of ungated populations are plotted. The ROI statistics corresponds to fluorescent EVs. Note the difference between the appearance of exs population from the same source (HEK 293 cells) stained with different dyes and/or prior or after isolation. (c) Histograms of SALS of EVs from (a). Left, histogram of EVs labeled during cell culture. Middle, histogram of differentially labeled MVs isolated from HEK293 cells. Right, histogram of differentially labeled exs isolated from HEK293 cells. F; S14 filtered through 0.22 µm filter; NF, S14 non-filtered.

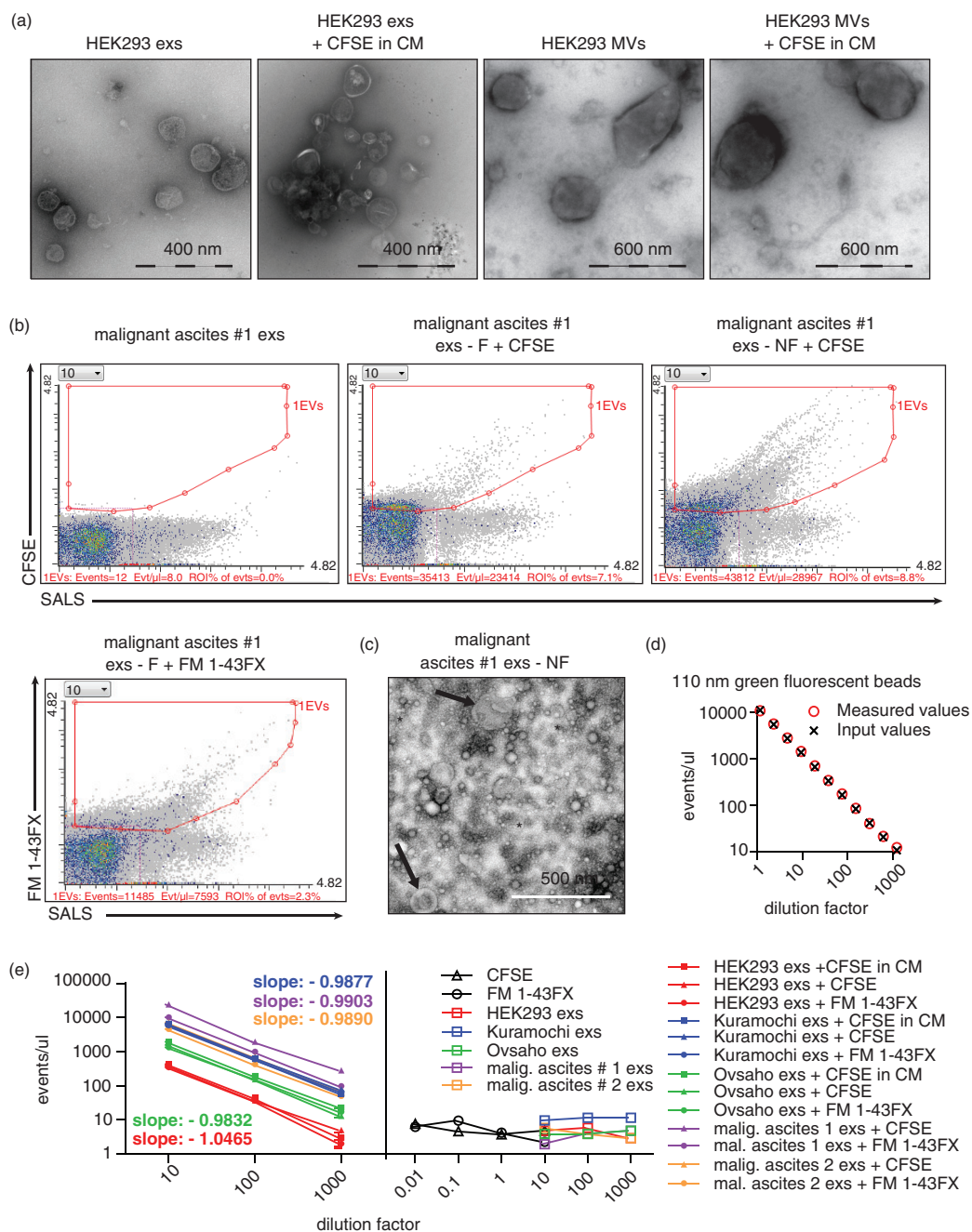


**Fig. 4.** Quantification of EVs by dedicated flow cytometer (FC). (a) Representative images of negatively contrasted exs and MVs from HEK293 cells (used in Fig. 3) visualized by TEM. The morphological characteristics are unchanged for EVs derived from HEK293 cells in the presence of 2  $\mu$ M CFSE in the CM. (b) Exs isolated from malignant ascites of ovarian cancer patients labeled by CFSE (upper middle and right panel), FM 1-43FX dye (lower left panel) and unlabeled (upper left panel). Note the difference between filtered (-F) and non-filtered (-NF) exs preparation. (c) Representative images of negatively contrasted exs from (b) visualized by TEM. Exs preparations isolated from malignant ascites of ovarian cancer patient #1 are contaminated by lipoprotein particles (smaller than exs, black asterisks) and sporadic MVs (larger than exs, black arrows), the latter are detected by FC also in (b). (d) Serial 2-fold dilutions of reference bead mix were measured using fluorescence threshold triggering. The measured values in ROI 2 (Fig. 1a) corresponding to 110-nm particles, (roughly reflecting exs) are plotted as red circles along with the calculated input amount of beads (X). Linear regression of log transformed data reveals slope  $-0.9954 \pm 0.0106$ ,  $R^2=0.9952$ . One representative experiment out of 3 is shown. (e) Quantification of exs from CM and patient samples. Left panel, event/ $\mu$ l for 10-fold dilutions of exs stained with CFSE in CM (indicated by squares), exs stained with CFSE prior to FC measurement (triangles) and exs stained with FM 1-43FX prior to FC measurement (spheres) were plotted against the dilutions. Slope/Y-intercept of linear regression analysis was calculated. Pooled slopes are presented for each source of exs indicated by color. Right panel, 10-fold dilutions of control samples (negative) indicate the background level of event/ $\mu$ l detected by FC.

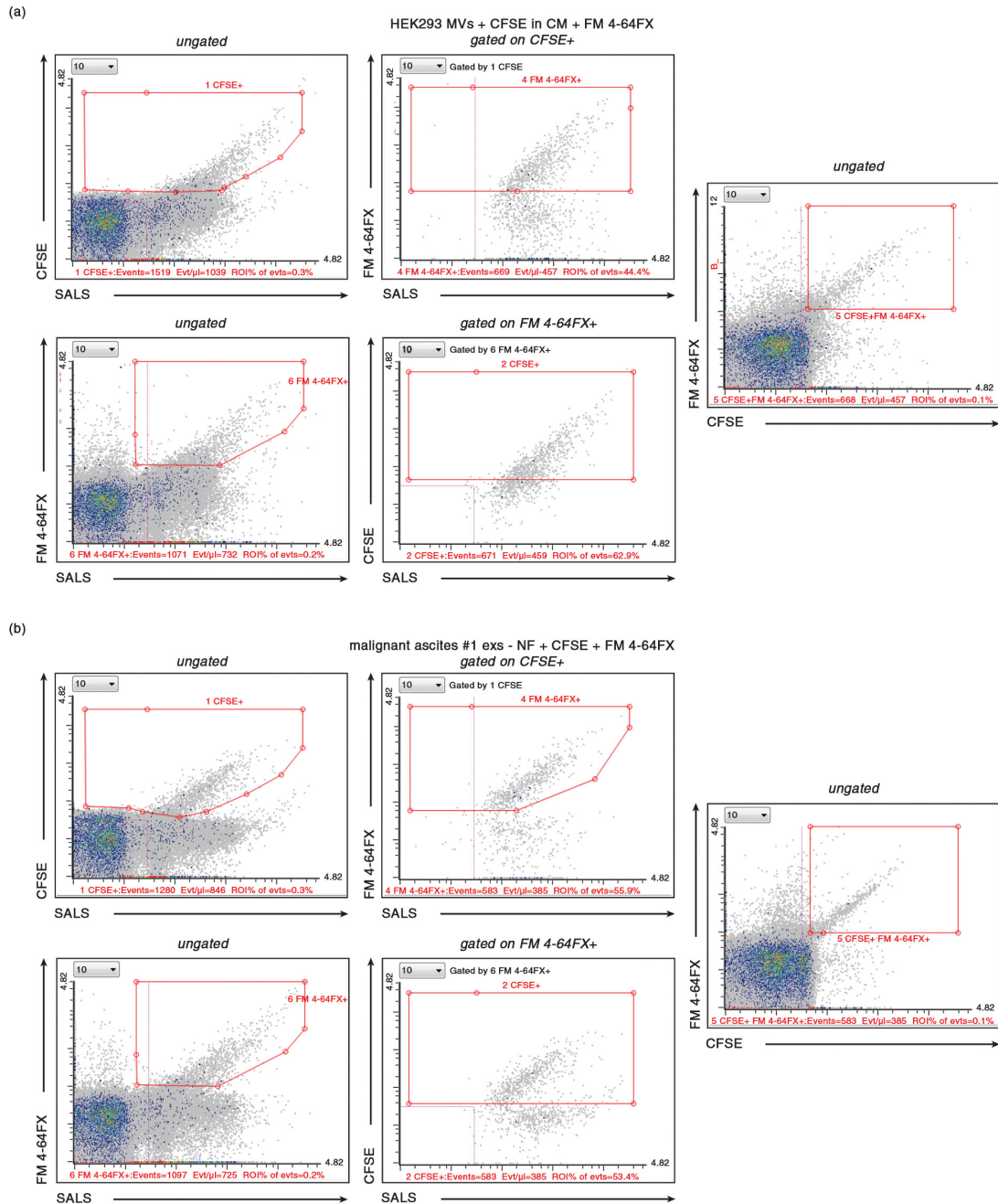


**Fig. 5.** Double labeling with protein- and lipid-specific dyes ensures precise enumeration of EVs. (a) MVs from HEK293 cells were pre-labeled during their biogenesis by CFSE in CM and post-labeled by FM 4-64FX dye. Upper cytograms show “CFSE<sup>+</sup> gating first” strategy, lower diagrams show “FM 4-64FX<sup>+</sup> gating first” strategy. The total amount of double positive MVs is the same in both strategies and equals the amount of EVs by direct gating for double positive MVs (right cytogram). (b) Exs from ascites of patient #1 were post-labeled by CFSE and FM 4-64FX dyes. Upper cytograms show “CFSE<sup>+</sup> gating first” strategy, whereas lower diagrams show “FM 4-64FX<sup>+</sup> gating first” strategy. The total amount of double positive MVs is the same in both strategies and equals the amount of EVs by direct gating for double positive MVs (right cytogram). – NF, 0.22  $\mu$ m non-filtered.

lipoprotein particles and also MVs (for TEM image see Fig. 4c). This experiment, however, provides proof of the principle that our methodology can also easily be applied to the complex samples of biological fluids and adapted for clinical use.

### *Dedicated FC represents a reliable method for the quantification of exs from different sources*

Based on the results in Figs. 1, 3, and 4 we concluded that our simplified isolation and labeling protocol combined with the dedicated FC (a) can easily distinguish

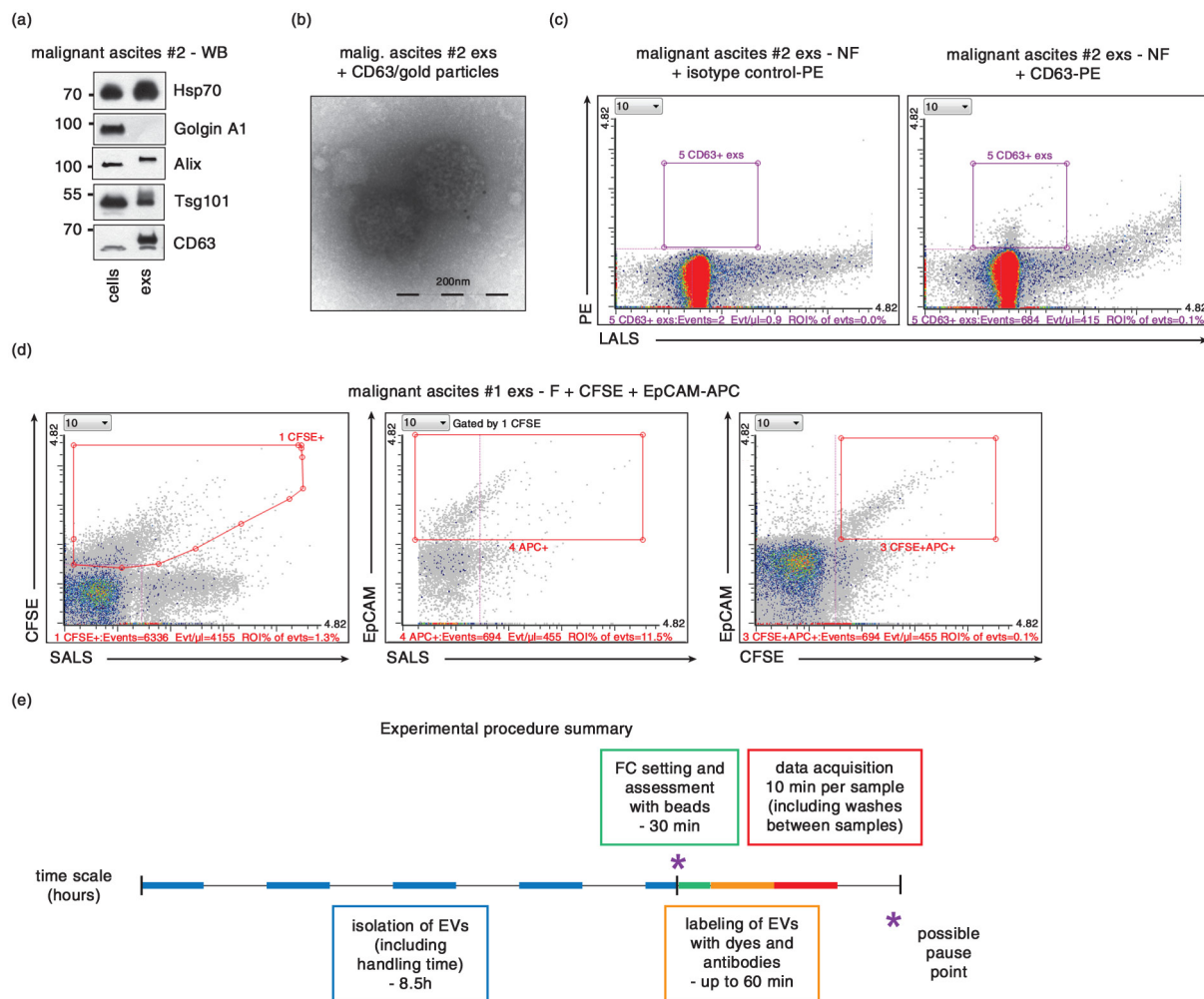


**Fig. 6.** Characterization of exs derived from ascites using antibodies. (a) Presence of characteristic exs markers Alix, Hsp70 and Tsg101 as well as CD63, and absence of “antimarker” Golgin A1 (present in the cells of origin but absent from exs) was verified by western blotting (WB) in cells (P 0.2 fraction) and exs from ovarian cancer patient #2. (b) TEM of exs isolated from ascites of ovarian cancer patient #2. Exs marker CD63 is detected at the surface of exs by secondary antibodies conjugated to 10-nm gold particles. (c) CD63<sup>+</sup> exs derived from ascites of ovarian cancer patient #2 can be detected by FC analysis of CD63-PE antibody-stained exs (right panel). Left panel, exs stained with isotype control antibody-PE. (d) Double labeling of exs from ascites of patient #1 by CFSE and EpCAM-APC antibody reveals feasibility of double labeling and demonstrates that only 11.5% of CFSE<sup>+</sup> exs are EpCAM<sup>+</sup>. (e) Summary of timing of the presented protocol. Each step is marked in the time scale by different color. For collection of EVs from conditioned media, cells are plated a day ahead. Isolation of exs can be achieved in 1 day. Setting up the instrument and FC data acquisition can be completed within the morning of the second day. – F, 0.22 μm filtered; – NF, 0.22 μm non-filtered.

fluorescently labeled exs from non-fluorescent background, (b) does not affect the morphological characteristics of exs, and (c) is applicable for analysis of exs from both relatively uniform cell line CM as well as complex clinical samples. So far, however, we did not evaluate the suitability of our approach for the quantitative analysis. To address this point, we first performed serial 2-fold dilutions of the reference bead mix and plotted the measured values of 110-nm fluorescent beads (events in ROI 2 in Fig. 1a) together with the calculated input based on the specified concentration of beads in the original solution of reference bead mix. The number of beads in

μl recorded in a fixed time frame (120 s) was plotted against the dilution factor of these beads and by linear regression we verified that the fluorescent microparticles of the approximate size of exs can be credibly quantified across wide range of concentrations (Fig. 4d). To determine the inter-sample variation, 3 individual tubes with identical reference bead mix dilutions were prepared and the mean ± standard error of the mean of 110-nm beads acquired within 120 s was calculated. The intra-sample variation was determined by quadruplicate measurements of the same beads dilution in 120-s time intervals. The inter- and intra-sample variations were relatively low, 7.0

and 1.4%, respectively, which demonstrates that dedicated FC has the potential to reliably quantify microparticles across several orders of magnitude.

Using serial dilutions, we also assessed performance of our protocol for exosomal preparations isolated from HEK293, other cell lines (Kuramochi and Ovsaho), and furthermore for the exs isolated from primary malignant ascites of 2 ovarian cancer patients. The results of this analysis are summarized in Fig. 4e. By linear regression and comparison of slopes and intercepts of the 2 or 3 lines of exs derived from the same source, we showed that numbers of recorded events/ $\mu\text{l}$  in dilutions corresponded well to the expected calculated ratios, as slopes of data from all individual samples were very close to the theoretically expected value -1.

This analysis also allowed us to compare individual labeling methods. First, the original amount of cells/CM and the dilution was the same for the exs labeled during the cell culture as was for the exs labeled prior to measurements. This indicates, that the short time labeling by CFSE prior to measurements (post-labeling) is as effective as the long-term cell labeling during their biogenesis in cell culture (pre-labeling). The prolonged exposure to CFSE, by which exs are believed to incorporate more CFSE, prior to and also after the release from cells, yielded equally brightly labeled vesicles as the typical CFSE labeling protocol, when the cells are labeled for 10 min in the tube and washed prior to seeding (data not shown). Second, the amount of events/ $\mu\text{l}$  recorded for exs+CFSE in CM were comparable to numbers of exs+CFSE and exs+FM 1-43FX with the maximal CV of 15.5% when different labeling approaches were compared. The fact that lipid-specific dye (FM 1-43FX) and protein-specific dye (CFSE) yield comparable numbers of fluorescently labeled exs isolated from CM of several cell lines (equal slopes and Y-intercepts) strongly indicates that the labeling is specific for exs, which contain both proteins and lipids. Slight differences between individual labeling techniques – with more exs consistently detected in CFSE-labeled samples (in comparison to FM 1-43FX) – were found in ascites-derived exs (CV of 33 and 22%). Such a discrepancy might be addressed by double labeling of EVs.

Thus, as a next step, we investigated whether we can double label the EVs with protein-specific and lipid-specific dyes. This approach would enable the separation of EVs from common contaminants of EV preparations, such as protein aggregates or micelles formed by unbound lipophilic styryl dyes, and explain the differences in EVs numbers obtained upon different labeling. We used CFSE and a variant of FM dye fluorescent in red spectrum – FM 4-64FX.

First, the EVs labeled during cell culture by CFSE were post-labeled with FM 4-64FX dye. Surprisingly, only 44% of CFSE<sup>+</sup> MVs were also positive for FM 4-64FX,

whereas 63% of FM 4-64<sup>+</sup> MVs were also positive for CFSE. Nevertheless, the total amount of double positive events recorded was the same regardless of the gating strategy – CFSE<sup>+</sup> first, FM 4-64FX<sup>+</sup> first, or double positive (Fig. 5a). We also noticed, that incubation of these CFSE pre-labeled EVs with FM 4-64FX dye greatly reduced their green fluorescence, resulting in non-detectable green fluorescence of HEK 293 exs (data not shown) and diminished green fluorescence of MVs, which was however still detectable and could be used for FC analysis (Fig. 5a). Thus, we post-labeled EVs with both CFSE and FM 4-64FX for 45 min at 37°C and showed, that in the case of exs isolated from malignant ascites, 56% of CFSE<sup>+</sup> exs were also positive for FM 4-64FX, whereas 54% of FM 4-64<sup>+</sup> MVs were also positive for CFSE. Similarly as in Fig. 5a, the total amount of double positive events was the same regardless of the gating strategy – CFSE<sup>+</sup> first, FM 4-64FX<sup>+</sup> first, or double positive (Fig. 5b).

This suggests that single labeling with CFSE may lead to overestimation of EV numbers; however, this overestimation is in the range of maximally tens of %, which is not ideal, but still much less than has been reported for other methods, such as NTA, which may overestimate the numbers of EVs in range of orders of magnitude (9,10).

#### *Dedicated FC is suitable for exosome characterization by antibody labeling*

For exs research it is not only important to enumerate the vesicles on single particle level but it is of vital importance to describe their further characteristics such as quantitatively and qualitatively assessing their protein composition and possible changes in protein abundance under various conditions. FC is ideal for precise and multiparameter characterization of EVs by staining with antibodies and detection by a fluorochrome. As a proof of principle of the suitability of the dedicated FC for this type of assay, we decided to evaluate expression of typical exs markers, tetraspanin CD63 (29), and EpCAM (30) on the exs derived from human ascites.

First, we analyzed biochemical composition of the exosomal sample by WB. This analysis showed positivity for typical exosomal markers (Alix, Hsp70, Tsg101, CD63) and negativity for “antimarkers” (Golgin A1), which are present in cells of origin but absent from isolated exs (Fig. 6a) (15,31,32). To further confirm presence of CD63 in the exosomal fractions of human ascites, we used immunolabeling with gold particles and were able to detect CD63 on the surface of exs (Fig. 6b).

Knowing that the exs from malignant ascites are CD63-positive, we decided to quantify the proportion of CD63<sup>+</sup> exosomes. We have used R-Phycoerythrin-(PE)-labeled primary antibody directed against CD63 antigen. PE and APC were chosen as fluorochromes due to their high quantum yields and extinction coefficients. Using this approach, we were able to show by the PE-labeled primary

antibody that exs isolated from malignant ascites of ovarian cancer patient #2 were CD63 positive (Fig. 6c). Based on the total amount of exs stained by CFSE in parallel tube, CD63<sup>+</sup> exs from malignant ascites made 38% of all CFSE<sup>+</sup> exs detected. Similarly, when we double stained the exs derived from ascites of patient #1 with CFSE and anti EpCAM antibody, we revealed that only 11% of CFSE<sup>+</sup> exs were positive for the cell adhesion molecule EpCAM (Fig. 6d), which has also been widely reported as an exs marker (30). Importantly, taken into account that single labeling with CFSE may overestimate the numbers of EVs as much as by 79%, the actual proportion of CD63<sup>+</sup> exs and EpCAM<sup>+</sup> exs may be up to 68 and 20%, respectively. This observation confirms previously anticipated, though poorly studied, variability among individual exosomal types and is consistent with our observations made by TEM, when only a fraction of ascites-derived exs stained with antimarker antibodies (Fig. 6b).

Taken together, our data demonstrate that exs and MVs from variant sources can be isolated, enumerated, and characterized via a standardized protocol and dedicated FC. Our protocol provides a fast – 10–12 h (Fig. 6e) – way to purify, quantify, and characterize EVs for both experimental as well as diagnostic purposes.

## Summary and conclusions

In the current study, we show that fluorescently labeled exs can be directly quantified and characterized using dedicated FC specifically designed for the analysis of small particles. The usefulness of dedicated FC for EV research was already demonstrated by others (13–15). Here we go further and present an analytical pipeline that does not require prior hardware adjustments of the device, which were needed for high-end conventional FC with the existing protocols (7,12). We show that EVs can be fluorescently labeled by combination of unspecific protein- and lipid-specific dyes and/or primary antibodies; staining can be performed either during cell culture or just prior to measurements. In the latter case, there is no need to remove the unbound fluorescent dye or fluorescently labeled antibody and after short incubation (5–45 min for dyes, 60 min if antibodies are used) data can be readily acquired. These properties allow implementing FC analysis directly into a routine, approximately 12 h workflow for purification and characterization of exs from both experimental and diagnostic samples.

We are aware of the fact that our approach is inferior to the existing exemplary FC protocol (7,12) in terms of purity and uniformity of obtained vesicular populations and their characteristics. Main advantages of our protocol are (a) its simplicity, (b) versatility, (c) minimal requirements on FC operator, and (d) short time required for analysis. As such it is suitable for and aimed at multiuser and clinical lab, where it has the potential to

bring desired level of control to the experiments involving exs and other small EVs. We believe that the ever-growing exosomal basic research may benefit from our protocol and the use of dedicated FC.

## Authors' contributions

VP and VB conceived and designed the research. VP, ZD, AK, and KK isolated the EVs and characterized them by WB. VP and JS acquired the FC data. DK, LI, and AH performed the electron microscopy experiments. IC, LM, and VW collected and EJ pathologically assessed the ascites samples. VP and VB interpreted the data and wrote the manuscript. Each author reviewed and made critical comments to the manuscript.

## Acknowledgements

We are grateful to Oliver Kenyon (Apogee Flow Systems) for technical support. We also thank Karel Nejedly and Karel Soucek (IBP CAS), Pavla Jendelova and Karolina Turnovcova (IEM CAS), and Ondrej Hovorka for technical equipment; Igor Cervenka (FS MUNI) for help with statistics; and Iva Kubikova for tips about TEM of EVs. We thank Pascale Zimmermann (KU Leuven) for anti Alix antibody.

## Conflicts of interest and funding

JS is also a technical assistant at the local distributor of Apogee Flow Systems – Bio-port Europe. No other conflicts of interest apply. This work was supported by Grant Agency of Masaryk University, project MUNI/M/1050/2013, as well as by Grant Agency of the Czech Republic, project GAP301/11/0747. VP and VB were supported by the Program of Employment of Newly Graduated Doctors of Science for Scientific Excellence (grant number CZ.1.07/2.3.00/30.0009) cofinanced from European Social Fund and the state budget of the Czech Republic. ZD is supported by the FP7 International Training Network WntsApp (code 608180).

## References

1. Thery C, Ostrowski M, Segura E. Membrane vesicles as conveyors of immune responses. *Nat Rev Immunol.* 2009;9: 581–93.
2. Raposo G, Stoorvogel W. Extracellular vesicles: exosomes, microvesicles, and friends. *J Cell Biol.* 2013;200:373–83.
3. Stoorvogel W, Kleijmeer MJ, Geuze HJ, Raposo G. The biogenesis and functions of exosomes. *Traffic.* 2002;3:321–30.
4. Bobrie A, Thery C. Exosomes and communication between tumours and the immune system: are all exosomes equal? *Biochem Soc Trans.* 2013;41:263–7.
5. Properzi F, Logozzi M, Fais S. Exosomes: the future of biomarkers in medicine. *Biomark Med.* 2013;7:769–78.
6. Johnsen KB, Gudbergsson JM, Skov MN, Pilgaard L, Moos T, Duroux M. A comprehensive overview of exosomes as drug delivery vehicles – endogenous nanocarriers for targeted cancer therapy. *Biochim Biophys Acta.* 2014;1846:75–87.
7. van der Vlist EJ, Nolte-t Hoen EN, Stoorvogel W, Arkesteijn GJ, Wauben MH. Fluorescent labeling of nano-sized vesicles released by cells and subsequent quantitative and qualitative analysis by high-resolution flow cytometry. *Nat Protoc.* 2012; 7:1311–26.

8. Dragovic RA, Gardiner C, Brooks AS, Tannetta DS, Ferguson DJ, Hole P, et al. Sizing and phenotyping of cellular vesicles using Nanoparticle Tracking Analysis. *Nanomedicine*. 2011; 7:780–8.
9. van der Pol E, Coumans FA, Grootemaat AE, Gardiner C, Sargent IL, Harrison P, et al. Particle size distribution of exosomes and microvesicles determined by transmission electron microscopy, flow cytometry, nanoparticle tracking analysis, and resistive pulse sensing. *J Thromb Haemost*. 2014;12: 1182–92.
10. Gardiner C, Ferreira YJ, Dragovic RA, Redman CW, Sargent IL. Extracellular vesicle sizing and enumeration by nanoparticle tracking analysis. *J Extracell Vesicles*. 2013;2:19671, doi: <http://dx.doi.org/10.3402/jev.v2i0.19671>
11. Witwer KW, Buzas EI, Bemis LT, Bora A, Lasser C, Lotvall J, et al. Standardization of sample collection, isolation and analysis methods in extracellular vesicle research. *J Extracell Vesicles*. 2013;2:20360, doi: <http://dx.doi.org/10.3402/jev.v2i0.20360>
12. Nolte-‘t Hoen EN, van der Vlist EJ, Aalberts M, Mertens HC, Bosch BJ, Bartelink W, et al. Quantitative and qualitative flow cytometric analysis of nanosized cell-derived membrane vesicles. *Nanomedicine*. 2012;8:712–20.
13. Chandler WL, Yeung W, Tait JF. A new microparticle size calibration standard for use in measuring smaller microparticles using a new flow cytometer. *J Thromb Haemost*. 2011; 9:1216–24.
14. Montoro-Garcia S, Shantsila E, Orenes-Pinero E, Lozano ML, Lip GY. An innovative flow cytometric approach for small-size platelet microparticles: influence of calcium. *Thromb Haemost*. 2012;108:373–83.
15. Théry C, Amigorena S, Raposo G, Clayton A. Isolation and characterization of exosomes from cell culture supernatants and biological fluids. *Curr Protoc Cell Biol*. 2006;Chapter 3:Unit 3.22.
16. Lyons AB. Divided we stand: tracking cell proliferation with carboxyfluorescein diacetate succinimidyl ester. *Immunol Cell Biol*. 1999;77:509–15.
17. Weston SA, Parish CR. New fluorescent dyes for lymphocyte migration studies. Analysis by flow cytometry and fluorescence microscopy. *J Immunol Methods*. 1990;133:87–97.
18. Bohren CF, Huffman DR. Absorption and scattering of light by small particles. New York: Wiley; 1998. 544 p.
19. Bryja V, Schulte G, Arenas E. Wnt-3a utilizes a novel low dose and rapid pathway that does not require casein kinase 1-mediated phosphorylation of Dvl to activate beta-catenin. *Cell Signal*. 2007;19:610–6.
20. van der Pol E, Hoekstra AG, Sturk A, Otto C, van Leeuwen TG, Nieuwland R. Optical and non-optical methods for detection and characterization of microparticles and exosomes. *J Thromb Haemost*. 2010;8:2596–607.
21. Lacroix R, Robert S, Poncelet P, Kasthuri RS, Key NS, Dignat-George F, et al. Standardization of platelet-derived microparticle enumeration by flow cytometry with calibrated beads: results of the International Society on Thrombosis and Haemostasis SSC Collaborative workshop. *J Thromb Haemost*. 2010;8:2571–4.
22. Shapiro HM. Practical flow cytometry. New York: Wiley-Liss; 2003.
23. van Manen HJ, Verkuijlen P, Wittendorp P, Subramaniam V, van den Berg TK, Roos D, et al. Refractive index sensing of green fluorescent proteins in living cells using fluorescence lifetime imaging microscopy. *Biophys J*. 2008;94:L67–9.
24. van der Pol E, van Gemert MJ, Sturk A, Nieuwland R, van Leeuwen TG. Single vs. swarm detection of microparticles and exosomes by flow cytometry. *J Thromb Haemost*. 2012;10: 919–30.
25. Momen-Heravi F, Balaj L, Alian S, Mantel PY, Halleck AE, Trachtenberg AJ, et al. Current methods for the isolation of extracellular vesicles. *Biol Chem*. 2013;394:1253–62.
26. Lotvall J, Hill AF, Hochberg F, Buzas EI, Di Vizio D, Gardiner C, et al. Minimal experimental requirements for definition of extracellular vesicles and their functions: a position statement from the International Society for Extracellular Vesicles. *J Extracell Vesicles*. 2014;3:26913, doi: <http://dx.doi.org/10.3402/jev.v3.26913>
27. Lamparski HG, Metha-Damani A, Yao JY, Patel S, Hsu DH, Ruegg C, et al. Production and characterization of clinical grade exosomes derived from dendritic cells. *J Immunol Methods*. 2002;270:211–26.
28. Kipps E, Tan DS, Kaye SB. Meeting the challenge of ascites in ovarian cancer: new avenues for therapy and research. *Nat Rev Cancer*. 2013;13:273–82.
29. Mathivanan S, Simpson RJ. ExoCarta: a compendium of exosomal proteins and RNA. *Proteomics*. 2009;9:4997–5000.
30. Runz S, Keller S, Rupp C, Stoeck A, Issa Y, Koensgen D, et al. Malignant ascites-derived exosomes of ovarian carcinoma patients contain CD24 and EpCAM. *Gynecol Oncol*. 2007; 107:563–71.
31. Ghossoub R, Lembo F, Rubio A, Gaillard CB, Bouchet J, Vitale N, et al. Syntenin-ALIX exosome biogenesis and budding into multivesicular bodies are controlled by ARF6 and PLD2. *Nat Commun*. 2014;5:3477.
32. Pant S, Hilton H, Burczynski ME. The multifaceted exosome: biogenesis, role in normal and aberrant cellular function, and frontiers for pharmacological and biomarker opportunities. *Biochem Pharmacol*. 2012;83:1484–94.